

# Identification of a Contact Region between the Tridecapeptide $\alpha$ -Factor Mating Pheromone of *Saccharomyces cerevisiae* and Its G Protein-Coupled Receptor by Photoaffinity Labeling<sup>†</sup>

L. Keith Henry,<sup>‡,§</sup> Sanjay Khare,<sup>||</sup> Cagdas Son,<sup>‡</sup> V. V. Suresh Babu,<sup>||</sup> Fred Naider,<sup>||</sup> and Jeffrey M. Becker<sup>\*,‡</sup>

Department of Biochemistry and Cellular and Molecular Biology, University of Tennessee, Knoxville, Tennessee 37996, and  
Department of Chemistry, College of Staten Island, Staten Island, New York 10314

Received October 17, 2001; Revised Manuscript Received March 7, 2002

**ABSTRACT:** *Saccharomyces cerevisiae* haploid cells communicate with their opposite mating type through peptide pheromones ( $\alpha$ -factor and **a**-factor) that activate G protein-coupled receptors (GPCRs). *S. cerevisiae* was used as a model system for the study of peptide-responsive GPCRs. Here, we detail the synthesis and characterization of a number of  $\alpha$ -factor (Trp-His-Trp-Leu-Gln-Leu-Lys-Pro-Gly-Gln-Pro-Met-Tyr) pheromone analogues containing the photo-cross-linkable group 4-benzoyl-L-phenylalanine (Bpa). Following characterization, one analogue, [Bpa<sup>1</sup>, Tyr<sup>3</sup>, Arg<sup>7</sup>, Phe<sup>13</sup>] $\alpha$ -factor, was radioiodinated and used as a probe for Ste2p, the GPCR for  $\alpha$ -factor. Binding of the di-iodinated probe was saturable ( $K_d = 200$  nM) and competable by  $\alpha$ -factor. Cross-linking into Ste2p was specific for this receptor and reversed by the wild-type pheromone. Chemical and enzymatic cleavage of the receptor/radioprobe complex indicated that cross-linking occurred on a portion of Ste2p spanning residues 251–294 which encompasses transmembrane domain 6, the extracellular loop between transmembrane domains 6 and 7, and transmembrane domain 7. This fragment was verified using T7-epitope-tagged Ste2p and a biotinylated, photoactivatable  $\alpha$ -factor. After cross-linking with the biotinylated photoprobe and trypsin cleavage, the cross-linked receptor fragment was revealed by both an anti T7-epitope antibody and a biotin probe. This is the first determination of a specific contact region between a Class IV GPCR and its ligand. The results demonstrate that Bpa  $\alpha$ -factor probes are useful in determining contacts between  $\alpha$ -factor and Ste2p and initiate mapping of the ligand binding site of this GPCR.

G protein-coupled receptors (GPCRs)<sup>1</sup> comprise 1 of the largest superfamilies of proteins with over 1000 members represented in the human genome alone (1, 2). One of the key steps in understanding the mechanisms of action of these diverse GPCRs is to elucidate the structure of their ligand binding sites. With this information in hand, the mechanism of activation of the GPCR can begin to be understood.

While there has been considerable data published on the GPCR ligand binding sites for biogenic amines (see 3 for a

review), much less information exists concerning the binding sites of peptide-responsive GPCRs. Recently, several reports have addressed this issue with the use of 4-benzoyl-L-phenylalanine-containing (Bpa) photoreactive chemical groups (4–10). Incorporation of Bpa into the first position of parathyroid hormone (PTH) and its use as a cross-linkable probe resulted in evidence that the N-terminal residue of PTH interacts with the extracellular end of transmembrane helix 6 of its receptor PTH1-Rc (11). A recent study by Mouldous et al. (8) investigating the interaction between the heptadecapeptide nociceptin and the opioid receptor-like (ORL1) GPCR made use of [Bpa<sup>10</sup>, Tyr<sup>14</sup>]nociceptin and found that the photoactivatable Bpa moiety cross-linked to a six amino acid fragment (amino acids 296–302). These studies and others using Bpa-containing peptides have allowed for the identification of interacting receptor fragments and in some cases even specific contact residues (5–7, 9). Identification of these cross-linked receptor fragments is a first but critical step in the elucidation of direct residue to residue contacts between ligand and receptor and has the potential to provide significant insight into the mechanism of activation of GPCRs by peptide ligands.

GPCRs can bind a variety of molecules including biogenic amines, peptides, and sugars. The unicellular yeast *Saccharomyces cerevisiae* contains two GPCRs used by haploid cells in the detection and response to peptide pheromones secreted

<sup>†</sup> This work was supported by Grants GM22086 and GM22087 from the National Institutes of Health and by a grant from the PSC–CUNY Awards Program.

\* Correspondence should be addressed to this author at the Department of Microbiology, University of Tennessee, M409 WLS, Knoxville, TN 37996. Phone: 865-974-3006. FAX: 865-974-0361. Email: jbecker@utk.edu.

<sup>‡</sup> University of Tennessee.

<sup>§</sup> Current address: Department of Pharmacology, Vanderbilt University, Nashville, TN 37232-6600.

<sup>||</sup> College of Staten Island.

<sup>1</sup> Abbreviations: AHA, aminoheptanoic acid; BNPS-skatole, 2-(2'-nitrophenylsulfenyl)-3-methyl-3'-bromoindolene; Bpa, 4-benzoyl-L-phenylalanine; BSA, bovine serum albumin; CNBr, cyanogen bromide; DIEA, diisopropylethylamine; ESI-MS, electron spray mass spectrometry; Fmoc, 9-fluorenylmethoxycarbonyl; GPCR, G protein-coupled receptor; HBTU, 2-(1H-benzotriazol-1-yl)-1,1,3,3-tetramethyluronium hexafluorophosphate; HOBt, N-hydroxybenzotriazole; Nle, norleucine; tBoc, *tert*-butoxycarbonyl; TAME, N- $\alpha$ -p-tosyl-L-arginine methyl ester; TFA, trifluoroacetic acid; Wang resin, (4-hydroxymethyl)phenoxy-methyl on 1% cross-linked polystyrene resin (bead).

by cells of the opposite mating type during sexual reproduction (see 12, 13 for reviews). One of these receptors, Ste2p, responds to the  $\alpha$ -factor peptide pheromone (WHWLQLK-PGQPMY) while the other receptor, Ste3p, responds to the posttranslationally modified  $\alpha$ -factor peptide (YIIKGVF-WDPAC[S-farnesyl]-OCH<sub>3</sub>).

The study of the pheromone receptors in *S. cerevisiae* has led to many critical findings concerning the biology of GPCRs, such as the discovery of the Regulator of G-protein Signaling (RGS) family of proteins (14, 15). Additionally, Ste2p serves as a model protein for the study of GPCRs, as (i) its transmembrane domains (TMDs) appear to be arranged similarly to those of other GPCRs, (ii) interactions between the fifth and sixth transmembrane domains appear to be critical for proper signal transduction to the G protein, and (iii) close packing of the fifth and sixth TMDs appears to be structurally similar to that of rhodopsin (16). All of these factors suggest that while most GPCRs do not share sequence homology, they do have strong structural and functional similarities. Therefore, elucidation of contact residues between receptor and ligand should provide insight into structure–function relationships in binding and activation of peptide-responsive GPCRs.

Here, we describe the synthesis and the chemical and biochemical characterization of two series of Bpa-containing  $\alpha$ -factor analogues. One of the analogues, [Bpa<sup>1</sup>, (<sup>125</sup>I)Tyr<sup>3</sup>, Arg<sup>7</sup>, Phe<sup>13</sup>] $\alpha$ -factor, was specifically cross-linked into the  $\alpha$ -factor binding pocket of Ste2p and used to determine direct contacts between the pheromone and the receptor. Biochemical analysis localized the cross-link site within residues 251–294 of the Ste2p receptor.

## MATERIALS AND METHODS

**Organisms.** *S. cerevisiae* DK102 [*MATa ste2::HIS3 bar1 leu2 ura3 lys2 ade2 his3 trp1*] transformed with pNED1-*[STE2]* (17) was used in binding studies and in the growth arrest assays of various  $\alpha$ -factor analogues. Strain LM23-3AZ [*MATa FUS1::lacZ bar1-I*] from Lorraine Marsh, Albert Einstein College of Medicine, New York, NY, was used in *FUS1-lacZ* gene induction assays. Strain BJ2168 [*MATa prc1-407 prb1-1122 pep4-3 leu2 trp1 ura3-52*] transformed with pNED1-*[STE2]* (17) and BJS21 [*MATa ste2::kan<sup>R</sup> prc1-407 prb1-1122 pep4-3 leu2 trp1 ura3-52*] transformed with pJL147 [*STE2-T7*] were used in cross-linking assays. Strain BJS21 was constructed by deleting *STE2* from strain BJ2168 using the kanamycin deletion cassette. pJL147 (a gift from J. Konopka, 16) encoded Ste2p containing the T7 epitope (Met-Ala-Ser-Met-Thr-Gly-Gly-Gln-Met-Gly) introduced between Ste2p residues 303 and 304. All strains used had similar binding of  $\alpha$ -factor. However, the BJ2168pNED and BJS21 strains lacked several peptidases, so they were used to increase the yield of Ste2p in experiments involving cross-linking.

**Chemical Reagents.** All reagents and solvents used for the solid-phase peptide synthesis of the photoactivatable peptides were analytical grade and were purchased from Advanced Chem Tech (Louisville, KY), VWR Scientific (Piscataway, NJ), or Aldrich Chemical Co. (Milwaukee, WI). High-performance liquid chromatography (HPLC) grade dichloromethane (CH<sub>2</sub>Cl<sub>2</sub>), acetonitrile (ACN), methanol (MeOH), and water were purchased from VWR Scientific and Fisher Scientific (Springfield, NJ).

**Synthesis of Bpa-Containing [*Nle*<sup>12</sup>] $\alpha$ -Factor Analogues.** Automated syntheses were carried out on an Applied Biosystem 433A peptide synthesizer (Applied Biosystem, Foster City, CA) using preloaded Wang resins (0.70 mmol/g, Advanced ChemTech) for most of the peptides. Two series of peptides were synthesized. In the first series, 4-benzoyl-L-phenylalanine (Bpa) was systematically used to replace the wild-type residue in all positions of the tridecapeptide except for Gly<sup>9</sup>. The latter residue was not replaced because previous studies had concluded that substitution of Gly<sup>9</sup> by an L-residue results in a marked decrease in activity and affinity (18, 19). In the second series of peptides, Tyr<sup>13</sup> was replaced by Phe, Bpa was substituted at either position 1, 3, or 5, and a Tyr residue was substituted at either position 1 or 3. The goal of the second series of analogues was to prepare a photo-cross-linkable peptide which could also be followed by autoradiography. In most peptides, L-norleucine (Nle), which is isosteric with L-methionine, was incorporated at position 12 to replace the naturally occurring L-methionine to prevent oxidation of the sulfur atom of this amino acid during peptide synthesis and purification. Replacement of Met by Nle was shown previously to result in an analogue with equal activity and receptor affinity to those of the native pheromone (20). Since all analogues have Nle in place of Met<sup>12</sup>, this residue is eliminated from the abbreviated names for simplicity. The 0.1 mmol FastMoc chemistry of Applied Biosystems was used for the elongation of the peptide chain with an HBTU/HOBt/DIEA-catalyzed, single coupling step using 10 equiv of protected amino acids for 30 min.

**Cleavage of Peptide.** The N- $\alpha$ -deprotected peptidyl resin was washed thoroughly with 1-methyl-2-pyrrolidinone and dichloromethane and dried in vacuo for 2 h. The peptide was cleaved from the resin support with simultaneous side chain deprotection using a cleavage cocktail containing trifluoroacetic acid (10 mL), crystalline phenol (0.75 g), thioanisole (0.5 mL), and water (0.5 mL) at room temperature for 1.5 h with the omission of 1,2-ethanedithiol in the cleavage reaction, because it was known to transform Bpa-containing peptides to cyclic dithioketal derivatives (21). The filtrates from the cleavage reaction were collected, combined with trifluoroacetic acid washes of the resin, concentrated under reduced pressure, and treated with cold ether to precipitate the crude product.

**Purification and Characterization.** The crude peptide so obtained was purified by reversed phase HPLC (Hewlett-Packard Series 1050) on a semipreparative Waters  $\mu$ -Bondapak C<sub>18</sub> (19  $\times$  300 mm) column with detection at 220 nm. The crude product (50 mg) was dissolved in about 4 mL of aqueous acetonitrile (20%) containing 0.025% TFA, applied to the column, and eluted with a linear gradient of water/acetonitrile containing 0.025% TFA (0–70% acetonitrile over 2 h at a flow rate of 5 mL/min). The fractions were collected and analyzed at 220 nm by reversed phase HPLC (Hewlett-Packard Series 1050) on an analytical Waters  $\mu$ -Bondapak C<sub>18</sub> (3.9  $\times$  300 mm) column. Fractions of over 99% homogeneity were pooled and subjected to lyophilization. The purity of the final peptide was assessed by analytical HPLC using two different solvent systems (10–55% acetonitrile gradient, 15 min, with 0.025% trifluoroacetic acid; and 50–80% methanol gradient, 30 min, with 0.025% trifluoroacetic acid), amino acid analysis (Biopoly-

mer lab, Brigham and Women's Hospital, Cambridge, MA), and electrospray ionization mass spectrometry (ESI-MS Peptido Genic Inc., Livermore, CA).

**Growth Arrest (Halo) Assay.** Solid MLT medium [yeast nitrogen base without amino acids (Difco), 6.7 g/L; casamino acids (Difco), 10 g/L; glucose, 20 g/L; adenine sulfate, 0.058 g/L; arginine, 0.026 g/L; asparagine, 0.058 g/L; aspartic acid, 0.14 g/L; glutamic acid, 0.14 g/L; histidine, 0.028 g/L; isoleucine, 0.058 g/L; leucine, 0.083 g/L; lysine, 0.042 g/L; methionine, 0.028 g/L; phenylalanine, 0.69 g/L; serine, 0.52 g/L; threonine, 0.28 g/L; tyrosine, 0.042 g/L; valine, 0.21 g/L; and uracil, 0.028 g/L] (27) was overlaid with 4 mL of *S. cerevisiae* DK102pNED cell suspension ( $2.5 \times 10^5$  cells/mL of Nobel agar). Filter disks (sterile blanks from Difco), 8 mm in diameter, were impregnated with 10  $\mu$ L portions of peptide solutions at various concentrations and placed onto the overlay. The plates were incubated at 30 °C for 24–36 h and then observed for clear zones (halos) around the disks. The data were expressed as the diameter of the halo including the diameter of the disk. A minimum value for growth arrest is 9 mm, which represents the disk diameter (8 mm) and a small zone of inhibition. All assays were carried out at least 3 times with no more than a 2 mm variation in halo size at a particular amount applied for each peptide. The values reported represent the mean of these tests.

**Effect of  $\alpha$ -Factor Analogues on Gene Induction.** *S. cerevisiae* LM23-3AZ carries a *FUS1* gene that is inducible by mating pheromone and which is fused to the reporter gene  $\beta$ -galactosidase. Cells were grown overnight in MLT at 30 °C to  $5 \times 10^6$  cells/mL, washed by centrifugation, and grown for one doubling at 30 °C. Induction was performed by adding 15  $\mu$ L of peptide at various concentrations to 135  $\mu$ L of concentrated cells ( $2 \times 10^8$  cells/mL) in a 96 well microtiter plate. The mixtures were placed at 30 °C with shaking for 2 h. After this time, cells were harvested by centrifugation, and each pellet was resuspended in Z-Buffer containing  $\beta$ -mercaptoethanol (22) and assayed for  $\beta$ -galactosidase production (expressed as Miller units) in triplicate. Each experiment was carried out at least 3 times with the results similar in each assay. As cells were suspended in liquid medium, any contribution of diffusion through agar potentially present in the halo assay was eliminated in the gene induction assay.

**Binding Competition Assay with [ $^3$ H] $\alpha$ -Factor.** This assay was performed using strain DK102pNED and tritiated  $\alpha$ -factor prepared by reduction of [dehydroproline<sup>8</sup>, Nle<sup>12</sup>] $\alpha$ -factor as described previously (20). In general, cells were grown at 30 °C overnight and harvested at  $1 \times 10^7$  cells/mL by centrifugation at 5000g at 4 °C. The pelleted cells were washed 2 times in ice-cold buffer [PPBi: 0.5 M potassium phosphate (pH 6.24) containing 10 mM TAME, 10 mM sodium azide, 10 mM potassium fluoride, 1% BSA (fraction IV)] and resuspended to  $4 \times 10^7$  cells/mL. The binding assay was started by addition of [ $^3$ H] $\alpha$ -factor and various concentrations of nonlabeled peptide (140  $\mu$ L) to a 560  $\mu$ L cell suspension so that the final concentration of radioactive peptide was  $6 \times 10^{-9}$  M (20 Ci/mmol). Analogue concentrations were adjusted using UV absorption at 280 nm and the corresponding extinction coefficients. After a 30 min incubation, triplicate samples of 200  $\mu$ L were filtered and washed over glass fiber filtermats using the Standard Cell Harvester (Skatron Instruments, Sterling, VA) and

placed in scintillation vials for counting. Each experiment was carried out at least 3 times with the results similar in each assay. Binding of labeled  $\alpha$ -factor to filters in the absence of cells was less than 20 cpm. The  $K_i$  values were calculated by using the equation of Cheng and Prusoff, where  $K_i = EC_{50}/(1 + [\text{ligand}]/K_d)$  (23).

**Synthesis of Iodinated  $\alpha$ -Factor Peptides.** Peptides were iodinated with Iodogen tubes from Pierce, Inc., using conditions recommended by the manufacturer. Briefly, Iodogen tubes were pre-wet with  $2 \times$  Tris Iodination Buffer (TIB: 50 mM Tris, pH 7.5, 0.8 M NaCl). The TIB was decanted, 100  $\mu$ L of fresh TIB was added directly to the bottom of the Iodogen tube, and either 10  $\mu$ L of Na<sup>127</sup>I (1.86 mg/mL) or 10  $\mu$ L of Na<sup>125</sup>I (100  $\mu$ Ci/ $\mu$ L, pH 10, ICN) was added and incubated for 15 min with gentle swirling every 30 s. Activated iodide was transferred to a siliconized microfuge tube containing 100  $\mu$ L of the peptide (0.5 mmol/L in TIB) and incubated for 20 min with gentle mixing every 30 s. Scavenging buffer (50  $\mu$ L at 10 mg/mL tyrosine in TIB) was added and incubated for 5 min with mixing at minutes 1 and 4. Following incubation, 1 mL of TIB containing 5 mM EDTA was added. The remaining unreacted iodine was separated from peptide using a Waters Sep-Pak C<sub>18</sub> minicolumn. The eluted products were separated by HPLC using water/acetonitrile/0.025% TFA with an acetonitrile percentage of 20–35% over 30 min at 1.4 mL/min on a Waters  $\mu$ Bondapak C<sub>18</sub> reversed phase analytical column ( $3.9 \times 300$  mm). <sup>127</sup>I-labeled peptides were quantitated by UV spectrophotometry using their extinction coefficients. Radioiodinated peptides were labeled using carrier-free Na<sup>125</sup>I, and the resulting monoiodinated peptides were quantitated by converting total dpm associated with the HPLC-purified peptide to millimoles of peptide using the specific activity of carrier-free Na<sup>125</sup>I (2159 Ci/mmol).

**Synthesis of [Bpa<sup>1</sup>, Lys<sup>7</sup>( $\epsilon$ -biotinyl- $\beta$ -alanyl)] $\alpha$ -Factor.** This analogue was synthesized by first adding Boc- $\beta$ -alanine hydroxysuccinimide ester and then hydroxysuccinimido biotin ester to [ $\alpha$ -Fmoc-Bpa<sup>1</sup>] $\alpha$ -factor that had been prepared by solid-phase peptide synthesis. Details of the synthesis will be reported elsewhere. After removal of all protecting groups, the final peptide was purified to near-homogeneity by reversed phase HPLC. Its molecular weight was determined by electron spray mass spectrometry to be 2028.0 (calcd 2028.35). This compound was a full agonist in the growth arrest assay and exhibited a binding affinity close to that of  $\alpha$ -factor.

**Binding Assays with <sup>125</sup>I-Labeled  $\alpha$ -Factor.** DK102 pNED1 cells (grown in MLT medium) (17) and DK102 cells (grown in MLT medium supplemented with tryptophan) were harvested at  $1 \times 10^7$  cells/mL by centrifugation and resuspended to  $6.25 \times 10^7$  cells/mL in PPBi buffer (pH 6.24) and placed at 4 °C. In competition binding assays, [Bpa<sup>1</sup>, (<sup>125</sup>I)Tyr<sup>3</sup>, Arg<sup>7</sup>, Phe<sup>13</sup>] $\alpha$ -factor ( $2.4 \times 10^{-9}$  M final concentration) was premixed with various concentrations of cold competitor. In saturation binding assays, radiolabeled  $\alpha$ -factor analogues were diluted with cold analogue to obtain the peptide concentrations used in the assay. Cells in PPBi were then added to peptide solutions to a final density of  $6.25 \times 10^6$  cells/mL and incubated for 45 min at room temperature. Following incubation, the suspension was transferred ( $3 \times 200$   $\mu$ L) to wells of a 0.45  $\mu$ m MultiScreen-HV, 96 well plate (Millipore MHVBN4510) preblocked with PPBi.



Samples were vacuum-filtered, washed with PPBi (2 × 200  $\mu$ L), and counted on an LKB-Wallac ClinGamma 1272 gamma counter. Using this methodology, nonspecific binding of radiolabeled peptide to the filter was at background levels. Specific binding was determined by subtracting counts associated with the DK102 (*ste2*) strain from counts bound to the DK102pNED1 (*STE2*) strain.

**Cross-Linking of [Bpa<sup>1</sup>, (<sup>125</sup>I)Tyr<sup>3</sup>, Arg<sup>7</sup>, Phe<sup>13</sup>] $\alpha$ -Factor to Ste2p.** BJ2168pNED1 membranes (220  $\mu$ g of protein) (17) were incubated with 975  $\mu$ L of PPBi buffer (with 0.1% BSA) in siliconized microfuge tubes for 10 min at ambient temperature. [Bpa<sup>1</sup>, (<sup>125</sup>I)Tyr<sup>3</sup>, Arg<sup>7</sup>, Phe<sup>13</sup>] $\alpha$ -factor (10 and 20 million cpm) was added, and the reaction was incubated for 2 h at room temperature with gentle mixing. The reaction mixture was aliquoted into 3 wells of a chilled 24 well plastic culture plate preblocked with PPBi (0.1% BSA). Separation of the reaction mixtures into separate wells kept the depth of the samples minimal (~2 mm) for efficient UV penetration of the sample. The samples were held at 4 °C and irradiated without the culture plate lid at 365 nm for 1 h at a distance of 12 cm in a Stratlinker (Stratagene, La Jolla, CA). Membrane samples were recombined in siliconized microfuge tubes and washed twice by centrifugation (14000g) with PPBi (0.1% BSA). Membrane pellets were dissolved in 2 × sample buffer (0.25 M Tris-HCl, pH 8.8, 0.005% bromphenol blue, 5% glycerol, 1.25%  $\beta$ -mercaptoethanol, 2% SDS). Samples were heated to 37 °C for 10 min and separated by SDS-PAGE (10% gel; 30 mA). In competition cross-linking experiments, cold  $\alpha$ -factor was added together with radioiodinated peptide. For subsequent receptor digestion analysis, the gel was exposed to a phosphorimager screen (STORM, Molecular Dynamics), and the band of radioactivity corresponding to Ste2p was excised and placed into dialysis tubing (15 000 molecular weight cutoff) with buffer (0.2 M Tris-acetate, pH 7.4, 1.0% SDS, 100 mM dithiothreitol). Electrophoresis was performed by placing dialysis tubing containing the gel in a horizontal electrophoresis chamber with running buffer (50 mM Tris-acetate, pH 7.4, 0.1% SDS, 0.5 mM sodium thioglycolate). Elution was carried out at 100 V for 3 h. The buffer in the dialysis tubing was transferred to a Millipore Ultrafree-15 centrifuge filter device (30 000 molecular weight cutoff) and concentrated by centrifugation. Concentrated sample was washed 3 times with 50 mM Tris-HCl, pH 7.5. Half of the sample was further treated with PNGaseF (Glyco) according to the supplier's instructions.

**Digestion of Cross-Linked Ste2p.** Cross-linked samples were digested with BNPS-skatole, CNBr, or trypsin. For BNPS-skatole digestions, samples were dissolved in 70% acetic acid, and approximately 10 mg of BNPS-skatole was added. For CNBr digestion, samples were dissolved in 70% formic acid, and a few crystals of CNBr were added. For trypsin digestion, samples were dissolved in trypsin digestion buffer (Promega), and 20  $\mu$ g of trypsin (Sequencing Grade modified trypsin, Promega) was added. All digestion reactions took place under nitrogen and complete darkness. After digestion, samples were dried by vacuum centrifugation, resuspended in 50  $\mu$ L of 0.5 M Tris, pH 8.25, and re-dried. BNPS-skatole and CNBr samples were then dissolved in Tris-tricine sample buffer from Novex (San Diego, CA) and run on 16% and 10–20% tricine gels (Novex). Trypsin-digested samples were dissolved in loading buffer (Invitro-

gen) and run on 12% Bis-tris gels with MES running buffer (Invitrogen). Gels were dried and exposed to a phosphor-imager screen for 1–4 days.

**Cross-Linking of Biotinylated  $\alpha$ -Factor to Ste2p-T7.** [Bpa<sup>1</sup>, Lys<sup>7</sup>( $\epsilon$ -biotinyl- $\beta$ -alanyl)] $\alpha$ -factor was used in cross-linking studies with strain BJS21-pJL147 membranes. Receptors cross-linked with the biotinylated probe as described above were digested with trypsin for 18 h with addition of fresh trypsin after 12 h at 30 °C. Digested samples were run on two separate gels (18% SDS-PAGE), transferred to Immobilon-P, and blocked with 5% milk-TBS for 1 h. One blot was probed with NeurtAvidin-HRP (Pierce Chemical) and detected with Western Lightning Chemiluminescence Reagent plus (WLCR+, PerkinElmer). The second blot was probed with T7-HRP antibody (Novagen) according to manufacturer's instructions, and detected by WLCR+.

## RESULTS

**Synthesis of  $\alpha$ -Factor Analogues.** The automated solid-phase synthesis of most of the  $\alpha$ -factor analogues yielded crude peptides which were 60–70% homogeneous. Lower purities (<50%) were observed with the peptides containing diiodoTyr. In previous studies, we obtained better incorporation of diiodotyrosine into  $\alpha$ -factor when arginine replaced lysine in the seventh position (24, 25). Therefore, all  $\alpha$ -factor analogues synthesized in this investigation contained Arg<sup>7</sup>. [Arg<sup>7</sup>] $\alpha$ -Factor was previously shown to have the same activity and binding affinity as  $\alpha$ -factor (20). The crude peptides were all purified by reversed phase HPLC to over 99% homogeneity based on analytical HPLC in both an acetonitrile/water/TFA and a methanol/water/TFA gradient system. All peptides were subjected to amino acid analysis and electrospray ionization mass spectrometry. Physicochemical data for peptides containing both Bpa and Tyr substitutions are summarized in Table 1. Similar characterization of the series containing only the Bpa substitution was also carried out (data not shown). Amino acid analysis and mass spectrometry verified the purity and composition of the synthetic  $\alpha$ -factor analogues used in this study.

**Receptor Affinities of Bpa-Scanned  $\alpha$ -Factor Analogues.** To attain efficient cross-linking of a ligand into a receptor binding site, it is necessary to employ ligands that bind tightly to the receptor. To ascertain the positions at which Bpa replacements would be tolerated, we scanned this residue throughout the peptide backbone. As seen in Figure 1, Bpa replacements at positions 1 (Trp), 3 (Trp), 5 (Gln), 7 (Lys), 8 (Pro), 12 (Met), and 13 (Tyr) were well tolerated, exhibiting decreases in  $K_d$  from 4-fold to 45-fold in comparison to  $\alpha$ -factor. In contrast, substitutions at positions 2, 4, 6, 10, and 11 resulted in 100-fold to greater than 1500-fold decreases in affinity. Based on these data and our working model for pheromone binding to receptor (26), analogues with Bpa at positions 1, 3, 5, and 13 were chosen for further evaluation as photo-cross-linkable  $\alpha$ -factors.

**Bioactivities of Iodinatable Bpa Analogues of  $\alpha$ -Factor.** To determine cross-link points between a ligand and its binding protein, tags are useful to reveal the covalent linkage point of the ligand. The most powerful tag available in terms of sensitivity is <sup>125</sup>I (27, 28). Previous studies showed that iodination of the C-terminal residue (Tyr<sup>13</sup>) resulted in biological inactivation of  $\alpha$ -factor (29). Another report by

Table 1: Physicochemical Properties of Photoactivatable Peptides

	peptides	MW <sup>a</sup>	MS <sup>b</sup>	K(a) <sup>c</sup>	K(b) <sup>c</sup>	amino acid analysis
1	Bpa <sup>1</sup> Y <sup>3</sup> R <sup>7</sup> Nle <sup>12</sup> F <sup>13</sup>	1720.03	1721.1	4.74	3.79	Y: 0.92(1); H: 0.93(1); L: 1.99(2); Q: 2.16(2); R: 0.89(1); P: 1.99(2); G: 0.99(1); Nle: 1.21(1); F: 0.98(1)
2	Y <sup>1</sup> Bpa <sup>3</sup> R <sup>7</sup> Nle <sup>12</sup> F <sup>13</sup>	1719.09	1720.3	4.61	2.99	Y: 0.91(1); H: 0.94(1); L: 1.98(2); Q: 2.13(2); R: 0.88(1); P: 1.97(2); G: 0.99(1); Nle: 1.23(1); F: 0.99(1)
3	Y <sup>1</sup> Bpa <sup>5</sup> R <sup>7</sup> Nle <sup>12</sup> F <sup>13</sup>	1779.12	1779.4	4.39	5.04	Y: 0.97(1); H: 0.81(1); L: 2.00(2); Q: 1.08(1); R: 0.96(1); P: 1.97(2); G: 0.99(1); Nle: 1.23(1); F: 0.99(1)
4	Y <sup>1</sup> R <sup>7</sup> Nle <sup>12</sup> Bpa <sup>13</sup>	1759.06	1760.0	5.19	3.83	Y: 0.95(1); H: 0.95(1); L: 1.95(2); Q: 2.11(2); R: 0.94(1); P: 1.92(2); G: 0.99(1); Nle: 1.19(1)
5	Bpa <sup>1</sup> (I <sub>2</sub> )Y <sup>3</sup> R <sup>7</sup> Nle <sup>12</sup> F <sup>13</sup>	1972.05	1973.0	4.15	4.92	Y: 0.82(1); H: 0.99(1); L: 2.01(2); Q: 2.18(2); R: 0.86(1); P: 1.94(2); G: 0.99(1); Nle: 1.23(1); F: 0.99(1)
6	(I <sub>2</sub> )Y <sup>1</sup> Bpa <sup>3</sup> R <sup>7</sup> Nle <sup>12</sup> F <sup>13</sup>	1972.21	1972.7	2.66	3.19	Y: 0.93(1); H: 0.97(1); L: 1.99(2); Q: 2.13(2); R: 0.92(1); P: 1.91(2); G: 0.96(1); Nle: 1.22(1); F: 0.98(1)
7	(I <sub>2</sub> )Y <sup>1</sup> Bpa <sup>5</sup> R <sup>7</sup> Nle <sup>12</sup> F <sup>13</sup>	2030.13	2030.7	2.92	5.56	Y: 0.91(1); H: 0.96(1); L: 1.99(2); Q: 1.08(2); R: 0.96(1); P: 1.93(2); G: 0.97(1); Nle: 1.21(1); F: 0.98(1)
8	(I <sub>2</sub> )Y <sup>1</sup> R <sup>7</sup> Nle <sup>12</sup> Bpa <sup>13</sup>	2011.08	2011.7	5.50	6.42	Y: 0.92(1); H: 0.89(1); L: 1.96(2); Q: 2.13(2); R: 0.89(1); P: 2.02(2); G: 0.97(1); Nle: 1.21(1)

<sup>a</sup> Calculated monoisotopic molecular weight. <sup>b</sup> Molecular mass determined using electron ionization mass spectroscopy (ESI-MS). <sup>c</sup> *K* is defined as  $(V_p - V_f)/V_f$  where  $V_p$  = the elution volume for the peptide and  $V_f$  = the breakthrough volume. *K*-values (a) were determined on a C<sub>18</sub>  $\mu$ -Bondpack column using a 10–55% acetonitrile gradient (0.025% trifluoroacetic acid) over 15 min and (b) were determined using 50–80% methanol gradient (0.025% trifluoroacetic acid) over 30 min.

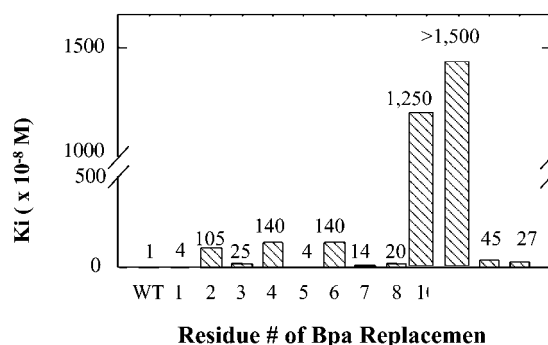


FIGURE 1: Binding affinity of Bpa-substituted  $\alpha$ -factor analogues. The binding affinities of Bpa-scanned  $\alpha$ -factor analogues were measured using [<sup>3</sup>H] $\alpha$ -factor and the binding competition assay described under Materials and Methods. The figure shows the calculated  $K_i$  (23) for each analogue. The numbers on the abscissa represent the position of the Bpa replacement. Each measurement was carried out at least 3 times with an error of not more than 10% for each value shown. The number above each bar represents the  $K_i$  value ( $\times 10^8$ ) of that analogue.

Masui et al. (30) suggested that Tyr<sup>13</sup> in  $\alpha$ -factor was essential and could not be substituted by other amino acids without loss of activity. However, it was recently demonstrated that Tyr<sup>13</sup> was replaceable by Phe with little to no effect on biological activity or binding affinity of  $\alpha$ -factor (25, 31). Therefore, we evaluated [Bpa<sup>x</sup>, Phe<sup>13</sup>] $\alpha$ -factor analogues (where  $x = 1, 3$ , or  $5$ ) and [Bpa<sup>13</sup>] $\alpha$ -factor analogues in which Tyr residues were substituted at other positions in these tridecapeptides. Based on the occurrence of Trp in positions 1 and 3 of the native  $\alpha$ -factor structure, we synthesized analogues 1–8 (Table 1).

Growth arrest assays and *FUS1* gene induction assays were performed to determine the biological activity of these analogues (Table 2). Semilogarithmic plots of halo diameter versus amount of peptide applied to the disk were all linear and exhibited similar slopes (data not shown). All analogues used in this assay were stable to enzymatic cleavage under the conditions tested as strains used in this analysis lacked the Bar1p protease that cleaves  $\alpha$ -factor. Therefore, the growth arrest data are indicative of the relative agonist activity of each peptide. The data show that peptides

Table 2: Biological Activity of  $\alpha$ -Factor Analogues

peptide (compound no.)	growth arrest <sup>a</sup> ( $\mu$ g of peptide)	<i>FUS1</i> -lacZ <sup>b</sup> induction potency (nM)	binding affinity, <sup>c</sup> $K_i$ (nM)
$\alpha$ -factor	0.4	3.1	9
Bpa <sup>1</sup> Y <sup>3</sup> R <sup>7</sup> F <sup>13</sup> (1)	1.0	4.4	127
Y <sup>1</sup> Bpa <sup>3</sup> R <sup>7</sup> F <sup>13</sup> (2)	inactive	149	157
Y <sup>1</sup> Bpa <sup>5</sup> R <sup>7</sup> F <sup>13</sup> (3)	> 10	184	150
Y <sup>1</sup> R <sup>7</sup> Bpa <sup>13</sup> (4)	inactive	inactive	132
Bpa <sup>1</sup> (I <sub>2</sub> )Y <sup>3</sup> R <sup>7</sup> F <sup>13</sup> (5)	1.5	14	199
(I <sub>2</sub> )Y <sup>1</sup> Bpa <sup>3</sup> R <sup>7</sup> F <sup>13</sup> (6)	7.3 <sup>d</sup>	19	216
(I <sub>2</sub> )Y <sup>1</sup> Bpa <sup>5</sup> R <sup>7</sup> F <sup>13</sup> (7)	> 10	26	22
(I <sub>2</sub> )Y <sup>1</sup> R <sup>7</sup> Bpa <sup>13</sup> (8)	inactive	33	315

<sup>a</sup> Values represent micrograms of peptide necessary to produce a halo with a diameter of 15 mm. Each assay was done in duplicate at least 3 times with a standard error of  $\pm 0.1$ . <sup>b</sup> Values represent nanomolar concentration of ligand to give 50% maximal activity in a *FUS1*-lacZ gene induction assay. Each assay was done in duplicate 3 times with a standard error of about 10% for each value shown. <sup>c</sup> Binding affinities were determined by calculation of  $K_i$  in competition binding assays using [<sup>125</sup>I]Y<sup>1</sup>R<sup>7</sup>F<sup>13</sup>] $\alpha$ -factor. Each assay was done in duplicate 3 times with a standard error of about 10% for each value shown. <sup>d</sup> The zone of growth inhibition was partially filled in, giving the halo a fuzzy appearance.

containing Bpa<sup>1</sup> with either Tyr<sup>3</sup> (compound 1) or (I<sub>2</sub>)Tyr<sup>3</sup> (compound 5) retain good agonist activity, requiring about 2.3-fold and 4-fold more of the pheromone derivative, respectively, to trigger the receptor. In contrast, tyrosinated analogues with Bpa<sup>3</sup> (2 and 6), with Bpa<sup>5</sup> (3 and 7), or with Bpa<sup>13</sup> (4 and 8) had little or no activity in the growth arrest assay. In the solution-phase, gene induction assay, compound 1 caused 50% of the maximal gene induction at only 33% higher concentration than  $\alpha$ -factor, and compound 5 required a 4-fold higher concentration. These results correlated with those of the growth arrest assay. Several of the peptides that were not active at the highest tested amount (10  $\mu$ g/disk) in the halo assay were agonists in the gene induction assay. In fact, all four iodinated compounds (5–8) had comparable activities in this assay. None of the  $\alpha$ -factor analogues induced growth arrest or *FUS1*-lacZ activation in a mutant lacking Ste2p, confirming that the  $\alpha$ -factor receptor was required for the biological activity of these peptides. Overall the bioassays demonstrate that  $\alpha$ -factor analogues containing

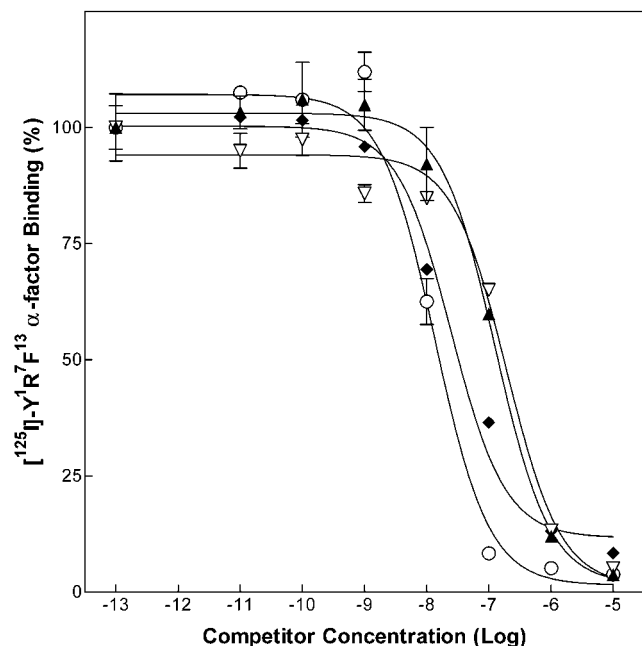


FIGURE 2: Competition binding assay of various  $\alpha$ -factor analogues vs [ $(^{125}\text{I})\text{Tyr}^1, \text{Arg}^7, \text{Phe}^{13}$ ] $\alpha$ -factor. Competitors were  $\alpha$ -factor (○), compound **1** (▲), compound **5** (▽), and compound **7** (◆).

both Bpa and iodotyrosine can induce Ste2p-dependent signaling.

**Binding Affinities of  $\alpha$ -Factor Analogues.** Binding affinities of the peptides were determined by competition and saturation binding assays as described under Materials and Methods. Representative competition binding data for  $\alpha$ -factor, and **1**, **3**, and **5** are presented in Figure 2. For most analogues, substitution of Bpa at positions 1, 3, 5, and 13 resulted in only 15–17-fold reduction in binding affinity versus native  $\alpha$ -factor (Table 2). With the exception of [ $(^{125}\text{I})\text{Tyr}^1, \text{Bpa}^5, \text{Arg}^7, \text{Phe}^{13}$ ] $\alpha$ -factor which showed increased binding, di-iodination of the Bpa analogues resulted in a slight reduction (1.5–2.4-fold) in binding compared to the noniodinated peptides.

**Iodination and Purification of  $\alpha$ -Factor Analogues.** Several of the Bpa-containing analogues were chosen for radioiodination based on the criteria that they had relatively good biological activity and binding affinities in the submicromolar range. [ $\text{Bpa}^1, \text{Tyr}^3, \text{Arg}^7, \text{Phe}^{13}$ ] $\alpha$ -Factor, [ $\text{Tyr}^1, \text{Bpa}^5, \text{Arg}^7, \text{Phe}^{13}$ ] $\alpha$ -factor, and [ $\text{Tyr}^1, \text{Arg}^7, \text{Bpa}^{13}$ ] $\alpha$ -factor were successfully iodinated, but the iodination of [ $\text{Tyr}^1, \text{Bpa}^3, \text{Arg}^7, \text{Phe}^{13}$ ] $\alpha$ -factor led to an unresolvable mixture (Figure 3B). This latter result is consistent with the recent observation that certain  $\alpha$ -factor analogues are resistant to iodination (25). As seen in Figure 3A, iodination of [ $\text{Bpa}^1, \text{Tyr}^3, \text{Arg}^7, \text{Phe}^{13}$ ] $\alpha$ -factor resulted in both the mono- and di-iodinated derivatives. The masses of the iodinated peptides were verified by electrospray mass spectrometry (data not shown). Based on the relatively high biological activity of [ $\text{Bpa}^1, \text{Tyr}^3, \text{Arg}^7, \text{Phe}^{13}$ ] $\alpha$ -factor (**1**) and its diiodinated homologue (**5**), the radio-iodinated form of this peptide was chosen for photolabeling of Ste2p.

**Competition of  $\alpha$ -Factor for [ $\text{Bpa}^1, (^{125}\text{I})\text{Tyr}^3, \text{Arg}^7, \text{Phe}^{13}$ ] $\alpha$ -Factor Binding to Ste2p.** [ $\text{Bpa}^1, (^{125}\text{I})\text{Tyr}^3, \text{Arg}^7, \text{Phe}^{13}$ ] $\alpha$ -Factor was shown to be displaced from Ste2p by  $\alpha$ -factor in a competition binding assay (Figure 4). The amount of bound peptide was expressed in dpm and plotted

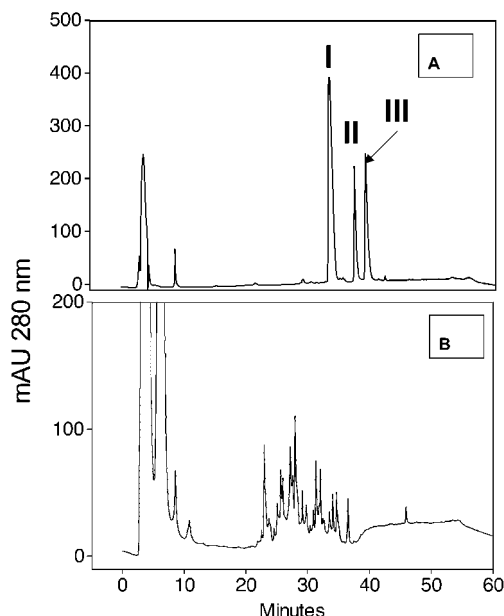


FIGURE 3: HPLC analysis of products from iodination of tyrosine-substituted  $\alpha$ -factor analogues.  $\alpha$ -Factor analogues were chemically iodinated using Iodogen reagent and products separated by HPLC. (Panel A) Iodination of [ $\text{Bpa}^1, \text{Tyr}^3, \text{Arg}^7, \text{Phe}^{13}$ ] $\alpha$ -factor: I, noniodinated peptide; II, mono-iodinated peptide; III, di-iodinated peptide. (Panel B) Iodination of [ $\text{Tyr}^1, \text{Bpa}^3, \text{Arg}^7, \text{Phe}^{13}$ ] $\alpha$ -factor.

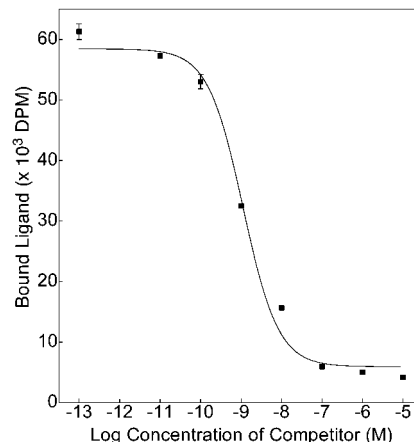


FIGURE 4: Competition binding of [ $(^{125}\text{I})\text{Bpa}^1, \text{Tyr}^3, \text{Arg}^7, \text{Phe}^{13}$ ] $\alpha$ -factor by nonradiolabeled  $\alpha$ -factor. Data were analyzed using a single-site competition binding equation. Error bars on some points are contained within the symbol and cannot be seen.

against the amount of cold competitor added. The binding competition was greater than 90%. The shape of the curve is consistent with competitive binding inhibition, indicating the radioligand is specific for Ste2p. Similar results were also obtained with [ $\text{Bpa}^1, (^{125}\text{I})\text{Tyr}^3, \text{Arg}^7, \text{Phe}^{13}$ ] $\alpha$ -factor, the di-iodinated form of this photoactivatable peptide (data not shown).

**Cross-Linking of [ $\text{Bpa}^1, (^{125}\text{I})\text{Tyr}^3, \text{Arg}^7, \text{Phe}^{13}$ ] $\alpha$ -Factor to Ste2p.** Membranes were incubated with [ $\text{Bpa}^1, (^{125}\text{I})\text{Tyr}^3, \text{Arg}^7, \text{Phe}^{13}$ ] $\alpha$ -factor, and cross-linking was carried out using light at 365 nm. A portion (20  $\mu\text{L}$ ) of the reaction mixture was removed following irradiation and tested for incorporation of radioactivity by processing over Multiscreen durapore membranes (26). The radioactive counts of the samples with and without competitor reveal a 76% reduction in cross-linked product in the presence of 100-fold excess  $\alpha$ -factor (Figure 5). The remainder of the reaction mixture was



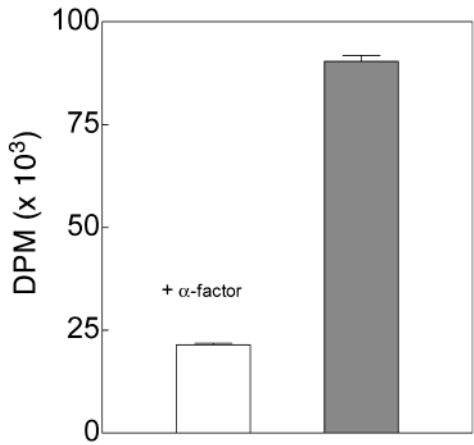


FIGURE 5: Total radioactive counts of [ $^{125}\text{I}$ ]Bpa<sup>1</sup>, Tyr<sup>3</sup>, Arg<sup>7</sup>, Phe<sup>13</sup>] $\alpha$ -factor bound to membranes following cross-linking in the presence and absence of nonradiolabeled  $\alpha$ -factor. Bars represent amount of ligand associated with membranes. Cross-linking was carried out in the presence (open bar) or absence (shaded bar) of nonlabeled  $\alpha$ -factor. The experiment was performed 3 times, and the error bars represent the variance observed.

analyzed by SDS-PAGE, and a cross-linked product (54 kDa) which migrated to the expected size of Ste2p (52 kDa) + probe (2 kDa) was detected by autoradiography (Figure 6). No cross-linked products were observed with samples that were not UV-irradiated (Figure 6, lanes 3 and 4). Co-incubation of membranes with radiolabeled probe and cold  $\alpha$ -factor resulted in a decrease in cross-linked product, showing that the cross-linking to Ste2p was specific (Figure 6, lane 1 vs lane 2). Western analysis using anti-Flag antibodies to detect Ste2p showed that all lanes had equivalent amounts of the receptor (data not shown).

**Fragmentation Analysis of Cross-Linked Ste2p.** Based on the specific cross-linking of [Bpa<sup>1</sup>, ( $^{125}\text{I}$ )Tyr<sup>3</sup>, Arg<sup>7</sup>, Phe<sup>13</sup>] $\alpha$ -factor to Ste2p, digestion of the receptor was initiated to identify the cross-linked fragment(s) of the receptor. Chemical cleavage with CNBr and BNPS-skatole was performed. These methods take place under strongly acidic conditions, which should result in unfolding of the receptor, thereby making it more accessible to cleavage (17). Chemical digestion of the receptor was carried out on native and deglycosylated Ste2p prepared by treatment of Ste2p with PNGaseF. Deglycosylation of the receptor was verified by SDS-PAGE with the deglycosylated receptor migrating with a molecular mass that was approximately 2 kDa smaller than the native receptor (data not shown). Similar results of deglycosylation of Ste2p were obtained previously by others (32, 33). In certain gels, Ste2p appeared as a diffuse band and sometimes appeared as a doublet. This is most likely due to the fact that strain BJ2168pNED1 expresses both a native chromosomal copy of *STE2* which codes for a 50 kDa protein when glycosylated, and an epitope-tagged, episomally expressed *STE2* which contains two epitope tags and codes for a 52 kDa protein when glycosylated.

BNPS-skatole, which cleaves at tryptophan residues, theoretically fragments the receptor into four pieces [IA: 9.5 kDa (7.5 kDa for residues 1–70 of Ste2p plus glycosyl groups of 2.5 kDa), IIA: 25 kDa (71–295), IIIA: 15 kDa (296–424), and IVA: 3.6 kDa (425–457)] (Figure 7A). Western analysis of native receptor with polyclonal antibodies against residues 1–60 revealed that, after a 2 min

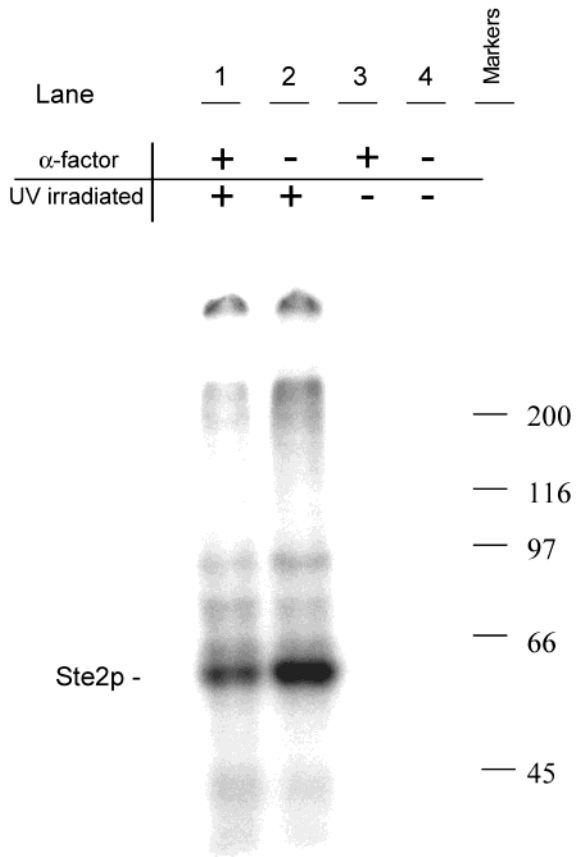


FIGURE 6: Autoradiogram of SDS-PAGE analysis of UV-irradiated DK102pNED membranes in the presence of [ $^{125}\text{I}$ ]Bpa<sup>1</sup>, Tyr<sup>3</sup>, Arg<sup>7</sup>, Phe<sup>13</sup>] $\alpha$ -factor. Membranes containing Ste2p were incubated with [ $^{125}\text{I}$ ]Bpa<sup>1</sup>, Tyr<sup>3</sup>, Arg<sup>7</sup>, Phe<sup>13</sup>] $\alpha$ -factor and irradiated at 365 nm as described under Materials and Methods. Control samples either were not irradiated or contained  $\alpha$ -factor as a competitor. Lane 1, UV irradiated plus 100-fold excess nonradiolabeled  $\alpha$ -factor; lane 2, UV irradiated; lane 3, 100-fold excess nonradiolabeled  $\alpha$ -factor without UV irradiation; lane 4, without excess nonradiolabeled  $\alpha$ -factor and without UV irradiation; lane 5, molecular weight markers.

incubation with the BNPS-skatole reagent, a broad band at approximately 35 kDa began to appear (Figure 8, lane B). The size of this band contains glycosylated and deglycosylated forms of a fragment consisting of residues 1–295 (fragments IA + IIA). After 24 h incubation with the BNPS-skatole reagent, two fragments of 7.5 and 9.5 kDa, corresponding to glycosylated and deglycosylated forms of fragment IA, were detectable (Figure 8, lane D) by a similar Western analysis. Thus, a 24 h incubation was required to ensure complete digestion of the Ste2p under the conditions used.

Ste2p containing cross-linked [Bpa<sup>1</sup>, ( $^{125}\text{I}$ )Tyr<sup>3</sup>, Arg<sup>7</sup>, Phe<sup>13</sup>] $\alpha$ -factor was digested for 24 h with BNPS-skatole, dissolved in tricine sample buffer, and run on gradient tricine gels. Phosphorimaging of the gels revealed two fragments of approximately 27 and 6 kDa (Figure 9, panel B). The 27 kDa fragment corresponds to that expected for complete BNPS-skatole cleavage of Ste2p (25 kDa fragment IIA, Figure 7A), plus 2 kDa for the probe. The 6 kDa fragment appears to be anomalous (see Discussion). In this gel and subsequent ones, an unidentified, low molecular weight form of radioactive iodine was readily discernible in the portion of the gel corresponding to a molecular size less than 4 kDa.

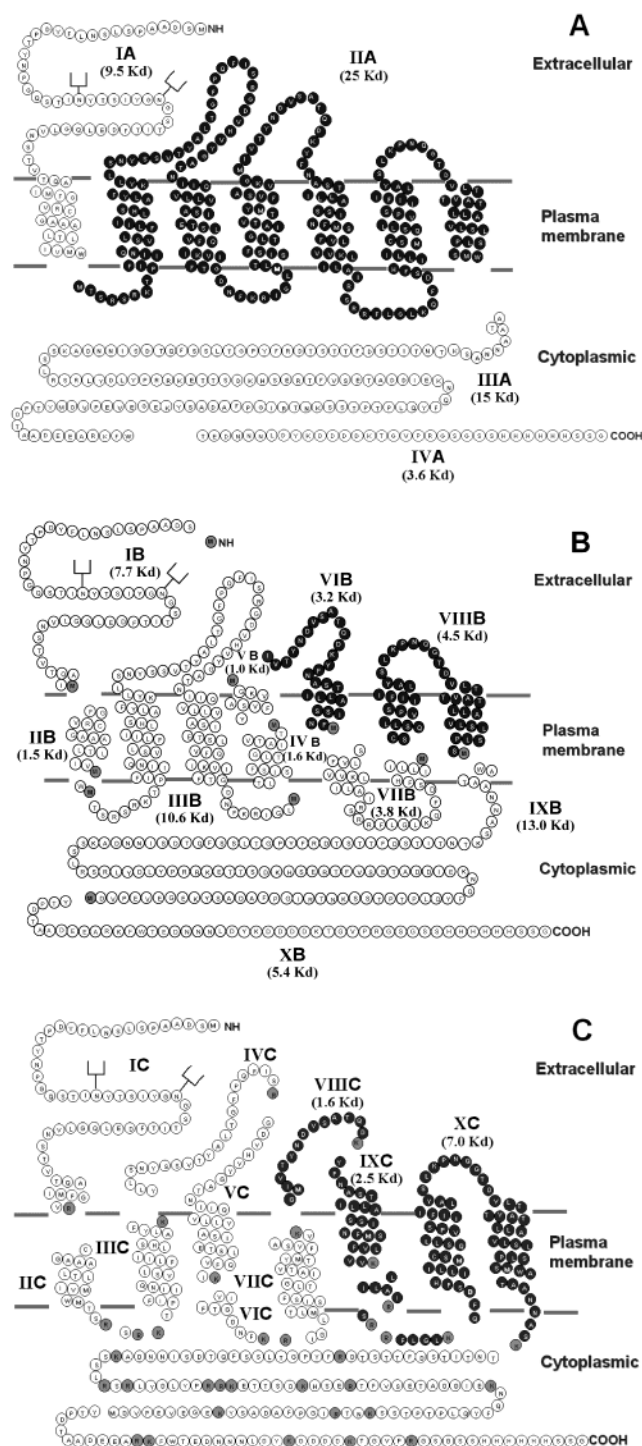


FIGURE 7: Schematic representation of chemical cleavage of Ste2p. These figures represent the BNPS-skatole, CNBr, and trypsin cleavage sites for the Ste2p receptor. Ste2p receptor is shown here using snake diagrams to represent the putative transmembrane domains. (Panel A) Cleavage of the receptor by BNPS-skatole results in four fragments labeled **IA** (residues 1–70 of Ste2p), **IIA** (71–295), **IIIA** (296–424), and **IVA** (425–458) with their respective molecular masses given in parentheses. Fragment **IA** contains the putative N-linked glycosylation sites as represented by the goalpost symbols. The oligosaccharides add 2 kDa of mass to fragment **IA**. Panel B represents the peptides resulting from a complete CNBr cleavage of Ste2p. Panel C represents the peptides resulting from a complete trypsin cleavage of Ste2p.

Complete cleavage of the cross-linked receptor with CNBr yielded one labeled fragment of ~6 kDa (Figure 10, panel I, lane B). Total cleavage of Ste2p labeled with [Bpa<sup>1</sup>,

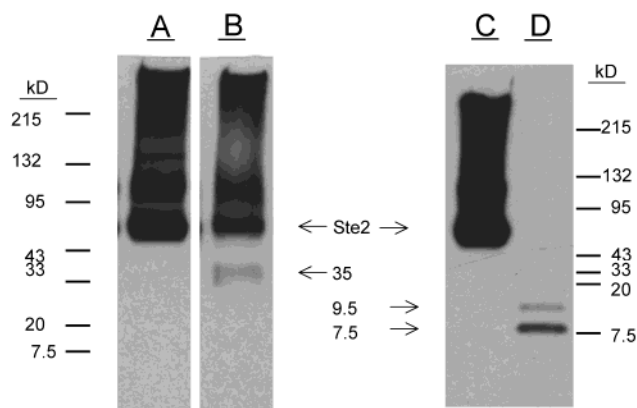


FIGURE 8: Western blot analysis of BNPS-skatole-digested membranes. Membranes were digested with BNPS-skatole, and at various time points, portions of the reaction mixture were removed and dried under vacuum centrifugation. Samples were then dissolved in tricine sample buffer and run on gradient tricine gels. Protein was transferred to Immobilon P membranes and probed with polyclonal antibodies specific for the first 60 amino acids of Ste2p. Lanes A and C were loaded with undigested membrane protein with intact Ste2p indicated in the figure. Lane B represents a 2 min digestion, and lane D shows a 24 h digestion with BNPS-skatole. The sizes of the detected fragments are indicated by arrows. Detected bands above 52 kDa are routinely observed in Western blot analysis of Ste2p and are widely believed to represent multimeric or aggregate structures of Ste2p (33).

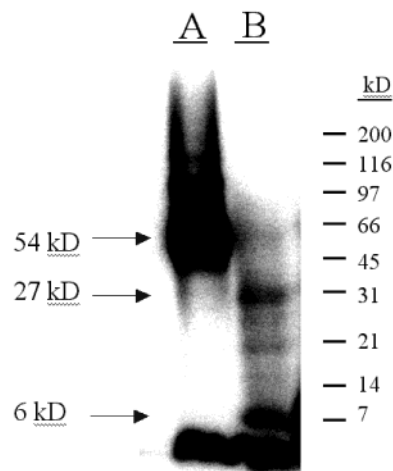


FIGURE 9: Autoradiograph of SDS-PAGE 10–20% tricine gel analysis of membranes photolabeled with [Bpa<sup>1</sup>, (<sup>125</sup>I)Tyr<sup>3</sup>, Arg<sup>7</sup>, Phe<sup>13</sup>] $\alpha$ -factor. (A) Photo-cross-linked membranes, untreated, and (B) photo-cross-linked membranes treated with BNPS-skatole and PNGaseF to remove N-linked oligosaccharides. Arrows denote cross-linked Ste2p receptor (lane A) and receptor fragments (lane B). Detected bands above 52 kDa are routinely observed in Western blot analysis of Ste2p and are widely believed to represent multimeric or aggregate structures of Ste2p (33).

(<sup>125</sup>I)Tyr<sup>3</sup>, Arg<sup>7</sup>, Phe<sup>13</sup>] $\alpha$ -factor could result in several possible radioactive fragments with a molecular mass of 6 kDa. Therefore, a partial CNBr digestion of cross-linked Ste2p was performed. This resulted in fragments of 35, 22, 9, and 6 kDa (Figure 10, panel II, lane B). All of these fragments can be rationalized in terms of theoretical CNBr cleavage points in Ste2p (Table 3). For example, the 35 kDa band (Figure 7B) could correspond to fragments **IVB** through **XB** (32.5 kDa) plus ligand (2 kDa). The smaller bands [23 (fragments **VIIIB**–**IXB** plus ligand), 10 (fragments **VIIIB**–**VIIIIB** plus ligand), and 6 kDa (fragment **VIIIB** plus ligand)] could all result from cleavages at Met residues within the



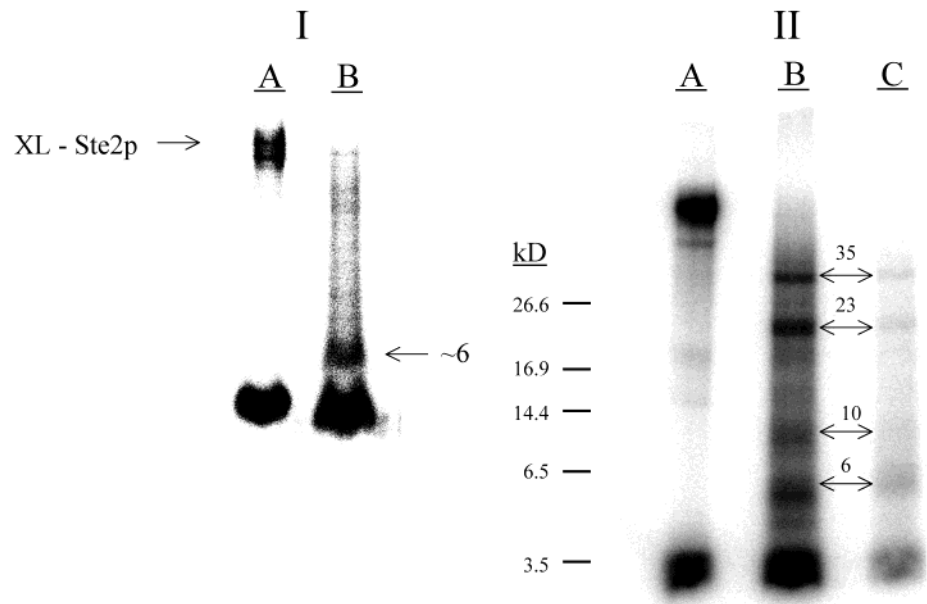


FIGURE 10: Autoradiographs of membranes photo-cross-linked with [Bpa<sup>1</sup>, (<sup>125</sup>I)Tyr<sup>3</sup>, Arg<sup>7</sup>, Phe<sup>13</sup>]α-factor and treated with cyanogen bromide run on an SDS–PAGE 10–20% tricine gel. I: lane A, photo-cross-linked membranes; lane B, complete digestion of photo-cross-linked membranes with CNBr. Arrows indicate photolabeled Ste2p and 6.7 kDa cleavage fragment of Ste2p. II: lane A, photo-cross-linked membranes; lane B, incomplete digestion of photo-cross-linked membranes; lane C, PNGaseF treatment of membranes from lane B.

Table 3: Peptides of CNBr-Digested Ste2p

peptide designation <sup>a</sup>	starting residue no. <sup>b</sup>	ending residue no. <sup>c</sup>	total no. of residues	molecular mass (Da)	accumulated molecular mass (kDa) <sup>d</sup>			
<b>IB</b>	2	54	53	5679	5.7	—	—	—
<b>IIB</b>	55	69	15	1521	7.2	1.5	—	—
<b>IIIB</b>	72	165	94	10621	17.8	12.1	10.6	—
<b>IVB</b>	166	180	15	1554	19.4	13.6	12.1	1.5
<b>VB</b>	181	189	9	1000	20.4	14.6	13.1	2.5
<b>VIB</b>	190	218	29	3227	23.6	17.8	16.3	5.7
<b>VIIB</b>	219	250	32	3774	27.4	21.6	20.1	9.5
<b>VIIIB</b>	251	294	44	4619	32	26.2	24.7	14.1
<b>IXB</b>	295	409	115	12962	45	39.2	37.7	27.1
<b>XB<sup>e</sup></b>	410	end	48	5407	50.4	44.6	43.1	32.5

<sup>a</sup> Peptides are named in order from the N-terminus to the C-terminus of Ste2p. Peptides of only one or two amino acids resulting from CNBr cleavage are not included in the table. <sup>b</sup> The residue within Ste2p of the first amino acid of this CNBr fragment. <sup>c</sup> The residue within Ste2p of the last amino acid of this CNBr fragment. <sup>d</sup> The total molecular mass of all fragments within a possible partial digest. For example, in the first column, fragments **IB** through **IIIB** have a molecular mass of 17.8 kDa. <sup>e</sup> The carboxyl terminus of Ste2p used in this study contained a His-tag and a FLAG tag (see Materials and Methods).

35 kDa peptide (Table 3). PNGaseF treatment of the mixture of fragments obtained by partial CNBr degradation did not result in any shifts in the band sizes (Figure 10, lane C). This was interpreted as ruling out fragment **IB** (glycosylated) in any of the cross-linked fragments detected.

Digestion of the cross-linked receptor with trypsin revealed one band of approximately 9 kDa corresponding to fragment **XC** (Figure 7C). It should be noted that cleavage at the Arg residue within the α-factor analogue does not occur because Arg is followed by a Pro residue. Cross-linking of ligand into **VIIIC** or **IXC** (Figure 7), two fragments of trypsin-hydrolyzed Ste2p that could correspond to fragments of CNBr-digested Ste2p, would have led to a much smaller band of radioactivity (approximately 3.5–4.5 kDa). Taken together, examination of all the digestion maps [BNPS-skatole (Figure 7A), CNBr (Figure 7B), and trypsin (Figure 7C)] indicated that the cyanogen bromide fragment **VIIIB** (Figure 7B, residues 251–294) was the smallest common cross-linked fragment. This portion of Ste2p corresponds to transmembrane domain 6, the extracellular loop between

transmembrane domains 6 and 7, and transmembrane domain 7.

The position of cross-linking of Ste2p and the probe was further examined using an epitope-tagged Ste2p (Ste2p-T7) and biotinylated, photoactivatable [Bpa<sup>1</sup>, Lys<sup>7</sup>(ε-biotinyl-β-alanyl)]α-factor. The T7 epitope, introduced between residues 303 and 304 at the C-terminal end of the tryptic fragment that spans TMD6 and TMD7, was fully tolerated by Ste2p (16). Trypsin digestion of Ste2p-T7 results in fragments similar to the wild-type Ste2p receptor, but fragment **XC** (Figure 7C) is tagged with the T7 epitope (1.1 kDa), allowing identification of this receptor fragment by western blotting with anti-T7 antibodies. Ste2p-T7 was cross-linked with [Bpa<sup>1</sup>, Lys<sup>7</sup>(ε-biotinyl-β-alanyl)]α-factor, digested with trypsin (18 h, 30 °C), run on SDS–PAGE, and probed with T7 antibodies to detect the epitope or probed with NeutrAvidin to detect biotin of the cross-linked α-factor analogue (Figure 12). The 14 kDa band corresponds to a partial trypsin digestion product containing **IXC**, **IL3**, and **XC** (Figure 7C) covering TMD5–TMD7 plus the cross-linked ligand (2.0

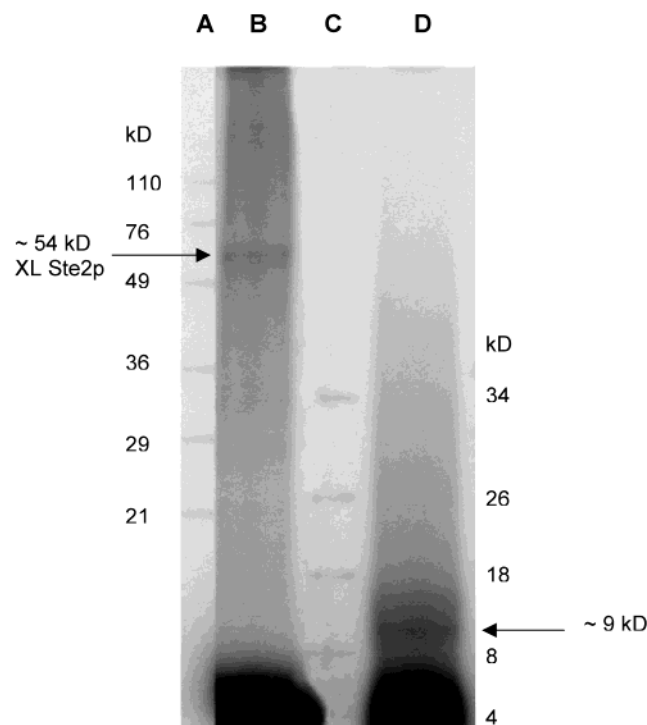


FIGURE 11: Autoradiogram of membranes photo-cross-linked with [Bpa<sup>1</sup>, (<sup>125</sup>I)Tyr<sup>3</sup>, Arg<sup>7</sup>, Phe<sup>13</sup>]α-factor and treated with trypsin run on SDS-PAGE 12% Bis-Tris with MES buffer. Lane B, cross-linked receptor before trypsin digestion; lane D, after trypsin digestion; lanes A and C, molecular mass markers with sizes indicated in the left and right margins.

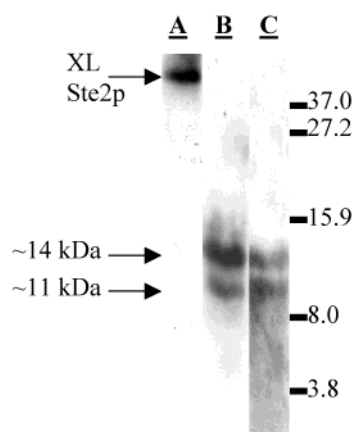


FIGURE 12: Western blot analysis of photo-cross-linked membranes. [Bpa<sup>1</sup>, K<sup>7</sup>(ε-biotinyl-β-alanyl)]α-factor was cross-linked into Ste2p-T7, treated with trypsin, and run on 18% SDS-PAGE. Lane A, before trypsin digestion probed with NeutrAvidin-horseradish peroxidase (NA-HRP); lane B, after trypsin digestion probed with NA-HRP; lane C, after trypsin digestion probed with anti-T7-HRP conjugate.

kDa) and the T7 epitope (1.1 kDa), and the 11 kDa band corresponds to fragment XC (Figure 7C) plus the cross-linked ligand and the T7 epitope. These fragments of cross-linked Ste2p-T7 were detected in lanes probed with either anti-T7 antibody or NeutrAvidin. In a parallel experiment (data not shown), the same two bands at 11 and 14 kDa were detected when a single gel blot was probed with anti-T7 antibody and then stripped and reprobed with NeutrAvidin. These results indicate that one fragment corresponding to XC contained the T7 epitope and the cross-linked [Bpa<sup>1</sup>, Lys<sup>7</sup>(ε-biotinyl-β-alanyl)]α-factor.

## DISCUSSION

Photoaffinity labeling with Bpa has been shown to be a useful tool in elucidating direct contacts between ligands and their cognate receptors (4–11). These photoaffinity studies, which include work on the parathyroid, secretin, and nociceptin receptors, have used receptor digestion analysis to elucidate fragments of the receptor that were cross-linked to the photoactivatable ligand probe. It should be noted, however, that receptor fragments may move anomalously on polyacrylamide gels and that molecular weights of small fragments are difficult to determine accurately. In favorable cases, specific residues involved in cross-linking were identified (5–7, 9). Site-directed mutagenesis studies can then be used to corroborate the importance of such residues in the binding of the ligand to the receptor.

The present study details the synthesis and testing of α-factor analogues containing Bpa for use as photoprobes to elucidate binding sites on the Ste2p receptor. Results from the Bpa-scanned α-factor series (Figure 1) allowed us to conclude that residues at positions 1, 3, 5, and 13 could be replaced with the photoactivatable amino acid without severe decreases in binding affinity. Based on previous structure–activity analyses (18–20, 24, 28–30), we then designed analogues containing iodinated tyrosine residues at positions 1 or 3 with phenylalanine at position 13. Bioassay and receptor binding studies indicated that these analogues triggered biological responses characteristic of Ste2p activation, and retained Ste2p-specific submicromolar binding affinities for this receptor (Table 2).

One of the analogues tested, [Bpa<sup>1</sup>, Tyr<sup>3</sup>, Arg<sup>7</sup>, Phe<sup>13</sup>]α-factor, was iodinated and exhibited relatively good agonistic activity in two standard pheromone response assays (growth arrest and *FUS1-lacZ*). Binding of [Bpa<sup>1</sup>, (<sup>125</sup>I)Tyr<sup>3</sup>, Arg<sup>7</sup>, Phe<sup>13</sup>]α-factor was found to be specific for the Ste2p receptor based on the ability of native α-factor to displace [Bpa<sup>1</sup>, (<sup>125</sup>I)Tyr<sup>3</sup>, Arg<sup>7</sup>, Phe<sup>13</sup>]α-factor in a competition binding assay (Figure 4). SDS-PAGE analysis of photolabeling experiments with [Bpa<sup>1</sup>, (<sup>125</sup>I)Tyr<sup>3</sup>, Arg<sup>7</sup>, Phe<sup>13</sup>]α-factor resulted in detection of one major radiolabeled product which migrated at the expected size of Ste2p covalently attached to the probe (54 kDa). The amount of 54 kDa product was reduced by >70% in the presence of excess cold α-factor, indicating that cross-linking was occurring at the pheromone binding site of Ste2p. These findings showed that the radioiodinated probe had biological and binding characteristics similar to native α-factor and cross-linked specifically to Ste2p. Thus [Bpa<sup>1</sup>, (<sup>125</sup>I)Tyr<sup>3</sup>, Arg<sup>7</sup>, Phe<sup>13</sup>]α-factor can be used to determine the binding site contacts between α-factor and its receptor.

Receptor cross-linked with the radiolabeled probe was purified by SDS-PAGE, eluted from the gel, and treated with various cleavage agents to identify a fragment(s) that covalently attached to the radioprobe. It was expected that cleavage at the Trp residues of Ste2p with BNPS-skatole would break the receptor into four fragments (Figure 8A: fragments IA, IIA, IIIA, and IVA). Previous studies by others have shown that the intracellular C-terminal tail of Ste2p has no effect on binding of α-factor and can actually be removed without loss of α-factor binding to Ste2p (32, 33). Based on this information, fragments IIIA and IVA were eliminated as possible sites for cross-linking as they make

up the intracellular C-terminal tail of the receptor and are not accessible to  $\alpha$ -factor. SDS-PAGE analysis with high percentage tricine gels resulted in identification of two major radiolabeled products of 27 and 6 kDa in size. The 27 kDa fragment corresponded to fragment **IIA** (25 kDa) plus the probe (2 kDa). The 6 kDa fragment was unexpected in that it does not correspond to a cross-linked form of fragment **IA** which would have an expected size of approximately 11 kDa (7.5 kDa + 2 kDa for the probe + 2 kDa for the polysaccharides = 11.5 kDa). The unexpected 6 kDa fragment most likely corresponds to cleavage of receptor fragment **IIA** at methionines and/or cysteines due to reagent contamination. It has been reported that slight impurities in BNPS-skatole can result in cleavage at methionines and cysteines (34). These impurities can arise from incomplete removal of *N*-bromosuccinimide (NBS) substrate during the synthesis of BNPS-skatole. However, NBS contamination is usually only a small fraction of the total reagent. As a result, Trp residues are cleaved fast by BNPS-skatole while the Met and Cys residues are cleaved at a slower rate. Based on this information, it is believed that the 6 kDa fragment was generated by cleavage at sites other than Trp in the 27 kDa fragment and would explain why the fragment was not detected in Western analysis by anti-N-terminal Ste2p antibodies following BNPS cleavage. This argument is strengthened by the observation that complete cleavage of Ste2p by CNBr at methionines also resulted in a 6 kDa fragment.

Complete cleavage of the cross-linked receptor with cyanogen bromide resulted in the identification of a single labeled band ~6 kDa in size. Based on the BNPS-skatole results, the band should be part of fragment **IIA** (Figure 7A). Complete CNBr cleavage of Fragment **IIA** should yield six fragments [**IIIB**: 10.6 kDa (residues 72–165 of Ste2p), **IVB**: 1.6 kDa (166–180), **VB**: 1.0 kDa (181–189), **VIB**: 3.2 kDa (190–218), **VIIB**: 3.8 kDa (219–250), and **VIIIB**: 4.5 kDa (251–294)] (Figure 7B). Of these, fragments **VIB**, **VIIB**, and **VIIIB** when cross-linked to the probe would give sizes similar to the identified radiolabeled fragment. Incomplete digestion of the cross-linked receptor with CNBr yielded four fragments (Figure 10, panel II, lane B). Digestion of the cross-linked receptor with trypsin revealed one band (Figure 11) of approximately 9 kDa corresponding to fragment **XC** (Figure 7C). Taken together, the results of the two chemical cleavages and trypsin cleavage indicated the receptor was labeled between residues 251 and 294. This portion of Ste2p corresponds to transmembrane domain 6, the extracellular loop between transmembrane domains 6 and 7, and transmembrane domain 7.

To verify that the 9 kDa fragment in Figure 11 was composed of a portion of Ste2p and the cross-linked  $\alpha$ -factor analogue, a receptor containing an epitope tag was utilized. This receptor, Ste2p-T7, carried the T7 epitope (Met-Ala-Ser-Met-Thr-Gly-Gly-Gln-Met-Gly) introduced between Ste2p residues 303 and 304. The epitope is thus N-terminal to a trypsin-sensitive Lys residue at position 304. In this manner, the **XC** fragment (Figure 7C) and any fragments resulting from partial digestion of Ste2p-T7 containing this portion of the receptor could be detected by antibody to T7. The Ste2p-T7 receptor was utilized successfully by Dube, De-Constanzo, and Konopka (16) previously to determine interactions between TMD5 and TMD6. Using Ste2p-T7

and a biotinylated, photoactivatable  $\alpha$ -factor analogue, [Bpa<sup>1</sup>K<sup>7</sup>( $\epsilon$ -biotinyl- $\beta$ -alanyl)] $\alpha$ -factor, we detected by anti-T7 antibody and by a biotin probe two bands at 11 and 14 kDa, corresponding respectively to **XC** with the T7 epitope plus the  $\alpha$ -factor and to **IXC-IL3-XC** with the T7 epitope and the  $\alpha$ -factor. The detection of both bands by the two probing methods indicated that the bands contained cross-linked [Bpa<sup>1</sup>K<sup>7</sup>( $\epsilon$ -biotinyl- $\beta$ -alanyl)] $\alpha$ -factor and a portion of Ste2p-T7. The increase in size from 9 kDa (Figure 11, Ste2p cross-linked to iodinated, photoaffinity probe) to 11 kDa (Figure 12, Ste2p-T7 cross-linked with biotinylated, photoaffinity probe) is consistent with the extra mass due to the  $\epsilon$ -biotinyl- $\beta$ -alanyl modification and the T7 epitope. These results strongly indicate that the region of the receptor cross-linked by a BPA<sup>1</sup>-photoactivatable probe, either iodinated or biotinylated, corresponded to residues 251–294 of Ste2p. The fact that the only two bands found on the SDS-PAGE gels were revealed by both epitope and biotin probes is strong evidence for the position of the cross-linking in the receptor. Although other 11 and 14 kDa fragments might occur during trypsin cleavage, they would not react with the anti-T7 antibodies.

The determination of a contact between the position 1 side chain of  $\alpha$ -factor and residues of Ste2p allows us to refine our current working model for the placement of  $\alpha$ -factor into the active site of this receptor. Based on site-directed mutagenesis and synthetic analogues, evidence was recently presented for a contact between the side chain of residue 10 (Gln) of  $\alpha$ -factor and residues 47 and/or 48 at the extracellular interface of the first transmembrane domain of the receptor (26). Fluorescence spectroscopy studies indicate that the side chain of Lys<sup>7</sup> most likely faces toward a pocket formed by the extracellular loops and that this pocket has both apolar and polar character (35). In addition, the side chain of Trp<sup>3</sup> is in a hydrophobic cavity based on fluorescence analyses (Ding, Becker, and Naider, unpublished results), and previous studies with position 1 analogues also indicate a strong preference for a large hydrophobic residue at the amino-terminal position of the pheromone (36). This latter result taken together with the present photolabeling analysis suggests that cross-linking occurs with residues that are at, or slightly below, the extracellular interface of transmembrane helices 6 and/or 7 of Ste2p. Finally, biophysical evidence exists supporting a bend around the Pro-Gly center of  $\alpha$ -factor as the biologically relevant conformation of the pheromone. In total, these results allow us to develop a crude two-dimensional model for fitting the tridecapeptide into the pheromone binding site. The working model has a contact of Gln<sup>10</sup> with residues S47 and/or T48, a contact of residues 1 and 3 with F262 and/or Y266, and a  $\beta$ -turn around the Pro-Gly sequence in the center of  $\alpha$ -factor. Recent studies indicate that F262 and Y266 are important for  $\alpha$ -factor binding and activity (Lee and Becker, unpublished results). Additional features of the bound structure should be forthcoming as we refine side chain contacts using the other photoactivatable analogues and site-directed mutagenesis studies currently in progress in our laboratory.

This study represents the first direct evidence of contact between the  $\alpha$ -factor ligand and a domain of the Ste2p receptor. Additionally, this is the first study to use Bpa photo-cross-linkable probes to study ligand-receptor interaction in class IV GPCRs. Future studies should allow for identi-



fication of a residue or residues that cross-link to the  $\alpha$ -factor probe used in this study. These results along with planned studies to use a series of  $\alpha$ -factor probes that will place cross-linkable moieties at various positions in the pheromone should allow for mapping of the ligand binding site of the Ste2p receptor. Results from such studies have the potential to provide key insight into peptide ligand mediated activation of GPCRs by identifying contact residues. Identification of the contact residues will allow us to begin assigning structure–function relationships between the  $\alpha$ -factor pheromone and Ste2p and compare the results to information gained from other classes of GPCRs.

## ACKNOWLEDGMENT

We thank Dr. James Konopka for the generous gifts of antibodies to the amino terminus of Ste2p and plasmid pJL147, Hui-Fen Lu and Shua-Hua Wang for technical help, Nathan VerBerkmoes for mass spectrometry analysis, and Drs. Melinda Hauser, Stephen Wright, and Byung-Kwon Lee for their insightful discussions.

## REFERENCES

- Venter, J. C., et al. (2001) *Science* 291, 1304–1351.
- Lander, E. S., et al. (2001) *Nature* 409, 860–921.
- Fong, T. M., and Strader, C. D. (1994) *Med. Res. Rev.* 14, 387–399.
- Dorman, G., and Prestwich, G. D. (2000) *Trends Biotechnol.* 18, 64–77.
- Dong, M., Wang, Y., Hadac, E. M., Pinon, D. I., Holicky, E., and Miller, L. J. (1999) *J. Biol. Chem.* 274, 19161–19167.
- Behar, V., Bisello, A., Rosenblatt, M., and Chorev, M. (1999) *Endocrinology* 140, 4251–4261.
- Hadac, E. M., Pinon, D. I., Ji, Z., Holicky, E. L., Henne, R. M., Lybrand, T. P., and Miller, L. J. (1998) *J. Biol. Chem.* 273, 12988–12993.
- Mouledous, L., Topham, C. M., Mazarguil, H., and Meunier, J. C. (2000) *J. Biol. Chem.* 275, 29268–29274.
- Boucard, A. A., Wilkes, B. C., Laporte, S. A., Escher, E., Guillemette, G., and Leduc, R. (2000) *Biochemistry* 39, 9662–9670.
- Shoelson, S. E., Lee, J., Lynch, C. S., Backer, J. M., and Pilch, P. F. (1993) *J. Biol. Chem.* 268, 4085–4091.
- Bisello, A., Adams, A. E., Mierke, D. F., Pellegrini, M., Rosenblatt, M., and Chorev, M. (1999) *Biochemistry* 38, 3414–3420.
- Blumer, K. J., and Thorner, J. (1991) *Annu. Rev. Physiol.* 53, 37–57.
- Dohlman, H. G., Thorner, J., Caron, M. G., and Lefkowitz, R. J. (1991) *Annu. Rev. Biochem.* 60, 653–688.
- Koelle, M. R. (1997) *Curr. Opin. Cell Biol.* 9, 143–147.
- Dohlman, H. G., Song, J., Ma, D., Courchesne, W. E., and Thorner, J. (1996) *Mol. Cell. Biol.* 16, 5194–5209.
- Dube, P., DeCostanzo, A., and Konopka, J. B. (2000) *J. Biol. Chem.* 275, 26492–26499.
- David, N. E., Gee, M., Andersen, B., Naider, F., Thorner, J., and Stevens, R. C. (1997) *J. Biol. Chem.* 272, 15553–15561.
- Shenbagamurthi, P., Kundu, B., Rath, S., Becker, J. M., and Naider, F. (1985) *Biochemistry* 24, 7070–7076.
- Abel, M. G., Zhang, Y. L., Lu, H. F., Naider, F., and Becker, J. M. (1998) *J. Pept. Res.* 52, 95–106.
- Rath, S. K., Naider, F., and Becker, J. M. (1988) *J. Biol. Chem.* 263, 17333–17341.
- Aletras, A., Barlos, K., Gatos, D., Koutsogianni, S., and Mamos, P. (1995) *Int. J. Pept. Protein Res.* 45, 488–496.
- Kippert, F. (1995) *FEMS Microbiol. Lett.* 128, 201–206.
- Cheng, Y., and Prusoff, W. H. (1973) *Biochem. Pharmacol.* 22, 3099–3108.
- Jiang, Y., Breslav, M., Khare, R. K., McKinney, A., Becker, J. M., and Naider, F. (1995) *Int. J. Pept. Protein Res.* 45, 106–115.
- Liu, S., Henry, L. K., Lee, B. K., Wang, S. H., Arshava, B., Becker, J. M., and Naider, F. (2000) *J. Pept. Res.* 56, 24–34.
- Lee, B. K., Khare, S., Naider, F., and Becker, J. M. (2001) *J. Biol. Chem.* 276, 37950–37961.
- Bitan, G., Scheibler, L., Greenberg, Z., Rosenblatt, M., and Chorev, M. (1999) *Biochemistry* 38, 3414–3420.
- Elliott, J. T., Hoekstra, W. J., Derian, C. K., Ahern, D. G., Addo, M. F., Maryanoff, B. E., and Prestwich, G. D. (2001) *J. Pept. Res.* 57, 454–506.
- Naider, F., and Becker, J. M. (1986) *CRC Rev. Biochem.* 21, 225–248.
- Masui, Y., Tanaka, T., Chinok, N., Kita, H., and Sakakibara, S. (1979) *Biochem. Biophys. Res. Commun.* 86, 982–987.
- Siegel, E. G., Gunther, R., Schafer, H., Folsch, U. R., and Schmidt, W. E. (1999) *Anal. Biochem.* 275, 109–115.
- Konopka, J. B., Jenness, D. D., and Hartwell, L. H. (1988) *Cell* 54, 609–620.
- Bukusoglu, G., and Jenness, D. D. (1996) *Mol. Cell. Biol.* 16, 4818–4823.
- Fontana, A. (1972) *Methods Enzymol.* 25, 419–423.
- Ding, F.-X., Lee, B. K., Hauser, M., Davenport, L., Becker, J. M., and Naider, F. (2001) *Biochemistry* 40, 1102–1108.
- Zhang, Y. L., Lu, H.-F., Becker, J. M., and Naider, F. (1997) *J. Pept. Res.* 50, 319–328.

BI015863Z